Original Article

Carcinogenic role of ESCO2 in cholangiocarcinoma: integration of bioinformatics analysis and experimental validation

Le Fan[1#^], Yong Jiang[1#^], Jing Hu[2^], Feng Xiao[1^], Yunxia Chai[1^], Bin Yi[1^], Yinghe Qiu[1^]

[1]Department of Organ Transplantation, the Third Affiliated Hospital of Naval Medical University (Oriental Hepatobiliary Surgery Hospital), Shanghai, China; [2]Department of Medical Imaging, Shanghai Yangpu District Shidong Hospital, Shanghai, China

Contributions: (I) Conception and design: L Fan, Y Jiang, B Yi, Y Qiu; (II) Administrative support: L Fan, Y Jiang, B Yi, Y Qiu; (III) Provision of study materials or patients: L Fan, Y Jiang, J Hu, F Xiao, Y Chai, B Yi, Y Qiu; (IV) Collection and assembly of data: L Fan, Y Jiang, J Hu, F Xiao, Y Chai; (V) Data analysis and interpretation: L Fan, Y Jiang, J Hu, F Xiao, Y Chai, B Yi, Y Qiu; (VI) Manuscript writing: All authors; (VII) Finalapproval of manuscript: All authors.

[#]These authors contributed equally to this work.

Correspondence to: Bin Yi, MD; Yinghe Qiu, MD. Department of Organ Transplantation, the Third Affiliated Hospital of Naval Medical University (Oriental Hepatobiliary Surgery Hospital), No. 700, Moyu North Road, Jiading District, Shanghai 201800, China.
Email: dfgdqgyz@163.com; qiuyinghe@aliyun.com.

Background: Cholangiocarcinoma (CCA) is a highly heterogeneous biliary malignancy with a poor prognosis. Finding early diagnosis and therapeutic targets for CCA is of great importance. The aim of this study was to screen for key genes involved in CCA using bioinformatics analysis, identify establishment of sister chromatid cohesion N-acetyltransferase 2 (*ESCO2*) as a core candidate, and validate its role experimentally.

Methods: The CCA data were downloaded using the Gene Expression Comprehensive Database and the Cancer Genome Atlas, the core gene *ESCO2* with strong correlation with CCA was screened by raw letter analysis, and the prognostic value of key CCA genes was analyzed by Kaplan-Meier. The effects of *ESCO2* on CCA cells and its oncogenic effects were investigated by cell and animal experiments.

Results: A total of 1,372 differential genes were screened in this study, with 742 up-regulated genes including *ESCO2* and 630 down-regulated genes. Patients with high *ESCO2* expression had a poorer prognosis and were significantly associated with N stage. Immune infiltration analysis revealed that *ESCO2* expression was negatively correlated with *CD8A* and *FGFBP2*. Cellular experiments showed that *ESCO2* was significantly up-regulated in CCA cells. *ESCO2* overexpression promotes CCA cell proliferation and inhibits apoptosis. *In vivo* experiments confirmed that *ESCO2* promotes tumor growth and shortens survival in mice.

Conclusions: *ESCO2* is a key regulatory gene affecting the development of CCA and plays an important role in CCA cell proliferation, which could be a new target for CCA diagnosis and treatment.

Keywords: Cholangiocarcinoma (CCA); establishment of sister chromatid cohesion N-acetyltransferase 2 (ESCO2); bioinformatics; prognosis; proliferation

Submitted Dec 02, 2025. Accepted for publication Mar 16, 2026. Published online Apr 23, 2026.
doi: 10.21037/tcr-2025-1-2695
View this article at: https://dx.doi.org/10.21037/tcr-2025-1-2695

^ ORCID: Le Fan, 0009-0009-8829-3904; Yong Jiang, 0009-0004-5462-5310; Jing Hu, 0009-0003-9354-9157; Feng Xiao, 0009-0002-0051-1794; Yunxia Chai, 0009-0000-0652-7143; Bin Yi, 0009-0001-6347-222X; Yinghe Qiu, 0009-0005-3309-0705.

Introduction

In recent years, cholangiocarcinoma (CCA), as the second largest hepatobiliary tumor after hepatocellular carcinoma, has shown a continuous rising trend in morbidity and mortality (1,2). CCA is a heterogeneous epithelial malignancy exhibiting multi-level heterogeneity, including intertumoral heterogeneity (such as differences in anatomical location, etiology, and molecular subtypes) and intratumoral heterogeneity (such as genetic, epigenetic, and phenotypic diversity among cancer cells within the same tumor). Due to its insidious onset and atypical early symptoms, most patients with CCA are in a progressive stage at the time of diagnosis and are not amenable to surgical treatment, while chemotherapy is rendered ineffective with drug resistance, with an extremely low median survival time and a 5-year survival rate of less than 20% (3,4). Therefore, the search for genetic drivers affecting the occurrence and progression of CCA is important for exploring molecular diagnostics and targeted therapies. However, the molecular mechanism of CCA is relatively complex, and the single most dominant signaling pathway has not yet been identified. Therefore, more and more biological analysis methods are applied to cancer research, and genomic and transcriptomic sequencing analyses can explore the pathogenesis of CCA at the molecular level.

Through the analysis of CCA tissue samples, the researchers found that many genes showed differential expression in tumor tissues and normal tissues, and these differentially expressed were involved in different signaling pathways, biological processes, or molecular functions (5). Analysis of differential signaling pathways helps to understand the status of the tumor as well as adopting targeted anti-tumor therapeutic regimens (6). In addition to this, data on gene expression can be used for typing tumor expression and also for assessing prognosis (7). Ma *et al.* (8) analyzed multiple bioinformatics datasets and found that AMDHD1, acting as a tumor suppressor, is downregulated in CCA and correlates with adverse clinical-pathological features and prognosis. Wang *et al.* (9) employed bioinformatics to reveal the upregulation and oncogenic role of STAMBPL1 in CCA. In this study, we found that establishment of sister chromatid cohesion N-acetyltransferase 2 (ESCO2) was significantly up-regulated in CCA and we investigated its biological function in CCA.

ESCO2 is an adhesin acetyltransferase consisting of a conserved C-terminal acetyltransferase structural domain, a C2H2 zinc finger structural domain, and a disordered region, of which its main function is to promote sister chromatid cohesion by acetylation of the cohesion-functioning subunit of structural maintenance of chromosomes 3 by the acetyltransferase structural domain (10). Mutations in the *ESCO2* gene can cause Roberts syndrome as well as mutations leading to mitotic failure (11). *ESCO2* has been found to be associated with the development and progression of a variety of malignant tumors (12,13). *ESCO2* is significantly upregulated in hepatocellular carcinoma tissues and is associated with poorer prognosis (14). *ESCO2* was able to promote malignant progression of head and neck squamous cell carcinoma (15). In addition, *ESCO2* is involved in regulating immune infiltration and influencing the prognosis of many cancers, especially bladder cancer, and may serve as a prognostic and immunotherapeutic biomarker for future human cancer treatments (16). However, studies and reports on *ESCO2* have not been seen in CCA.

The aim of this study was to retrieve the key genes of

Highlight box

Key findings

- This study provides the first discovery of the oncogenic role of establishment of sister chromatid cohesion N-acetyltransferase 2 (*ESCO2*) in cholangiocarcinoma (CCA).

What is known and what is new?

- *ESCO2* is an acetyltransferase involved in sister chromatid cohesion and has been implicated as an oncogene in various cancers, including hepatocellular carcinoma, head and neck squamous cell carcinoma, and renal cell carcinoma. It has been associated with prognosis, cell cycle regulation, and immune infiltration in pan-cancer analyses.
- This study provides the first comprehensive investigation of *ESCO2* in CCA. We newly identified that: (I) *ESCO2* is significantly upregulated in CCA tissues and cell lines; (II) high *ESCO2* expression is associated with poor prognosis and advanced N stage in CCA patients; (III) *ESCO2* expression shows a significant negative correlation with immune markers *CD8A* and *FGFBP2* in CCA; (IV) both *in vitro* and *in vivo* experiments functionally validate that *ESCO2* promotes CCA cell proliferation, invasion, and tumor growth while inhibiting apoptosis.

What is the implication, and what should change now?

- *ESCO2* is a key regulatory gene affecting the development of CCA and plays an important role in CCA cell proliferation, which could be a new target for CCA diagnosis and treatment. Further clinical validation is required in the future, and the downstream molecular mechanisms of *ESCO2* should be explored through in-depth molecular biology experiments.

CCA using Gene Expression Omnibus (GEO) and The Cancer Genome Atlas (TCGA), and to construct a protein interaction network by Gene Ontology (GO) function and Kyoto Encyclopedia of Genes and Genomes (KEGG) function analysis. The *ESCO2* gene was selected for its significantly upregulated expression in the analyzed datasets, and its biological relevance to cell cycle regulation and genomic stability has been confirmed in other tumors. We further screened and clarified the differential expression, prognostic value, and immune infiltration of the key gene *ESCO2*. Meanwhile, the oncogenic function of *ESCO2* was verified by *in vitro* and *in vivo* experiments to provide new biomarkers and therapeutic targets for the diagnosis of CCA. We present this article in accordance with the ARRIVE and MADR reporting checklists (available at https://tcr.amegroups.com/article/view/10.21037/tcr-2025-1-2695/rc).

Methods

Data sources and analysis

CCA data were downloaded from GEO (https://www.ncbi.nlm.nih.gov/geo/) and TCGA (https://portal.gdc.cancer.gov/), respectively. The GSE26566, GSE32225, and GSE132305 chip data sets were analyzed (Table S1). The GEOquery (17) and TCGAbiolinks (18) toolkits were used to download and process the GEO and TCGA data, and the sva (19) toolkit was used to remove batch effects. The study was conducted in accordance with the Declaration of Helsinki and its subsequent amendments.

Differential expression and pathway enrichment analysis

Differential expression analysis of CCA and paracancer data was performed by Limma (20,21) package and Ggplot2 package to obtain differential gene *ESCO2*. Similarly, high and low *ESCO2* expression groups were categorized according to the median value of *ESCO2*, after which differences were analyzed. *ESCO2* was then analyzed for GO function and KEGG pathway enrichment using the RclusterProfiler package ($P<0.05$) (22).

Correlation analysis of immune infiltration

Immunoinfiltration analysis of the relationship between *ESCO2* expression and immunoinfiltrating cells was performed using the MCPcounter algorithm (23,24).

Survival analysis and correlation with clinicopathologic parameters

Patients with CCA in TCGA were filtered to assess the prognostic impact of *ESCO2* expression. Clinicopathologic parameters with clear results for all samples. Parameters containing UNKNOWN or null values were excluded. Prognostic receiver operating characteristic (ROC) curves for *ESCO2* were constructed by the survival ROC package, including 1-, 3-, and 5-year ROC curves. Survival analysis of *ESCO2* was also performed to construct Kaplan-Meier survival plots, including overall survival (OS), disease-specific survival (DSS), disease-free interval (DFI), and progression-free survival (PFS). *ESCO2* expression was then analyzed in relation to clinicopathological parameters, including age, gender, and stage.

Construction of protein-protein interaction (PPI) networks and acquisition of key sub-networks

The PPI network of *ESCO2*-related differentially expressed genes was constructed based on the search tool for the retrieval of interaction gene/proteins (STRING) (25) database, and a connectivity of 0.7 was selected. Network visualization was also performed through Cytoscape (26) and key sub-modules were extracted with the help of molecular complex detection (23).

Copy number variation (CNV) mutation analysis of ESCO2

The relationship between *ESCO2* mRNA expression and CNV copy number mutations was analyzed using the CbioPortal database (27).

Cell culture

Human bile duct epithelial cells HIBEC (YS2223C) and human CCA cells: SK-ChA-1 (FY-FN3223), CCLP-1 (YS2074C), SNU-869 (JNO17-300), HuH-28 (YS1591C) were purchased from Shanghai Yaji Biotechnology Co., Ltd. HIBEC, SK-ChA-1, and CCLP-1 cells were cultured (37 ℃, 5% CO_2) using DMEM medium (Biogradetech, A-CSH795, Massachusetts, USA), while SNU-869 and HuH-28 cells were cultured in RPMI 1640 medium (Biogradetech, A-CSH790). When the cell growth fusion reached 80%, in the logarithmic growth phase and in good growth status, the cells were passaged in a 1:4 ratio for subsequent experiments.

Plasmid construction and cell transfection

Overexpression ESCO2 plasmid (miR-ESCO2), silencing ESCO2 plasmid (sh-ESCO2), overexpression control plasmid (miR-NC), and silencing control plasmid (sh-NC) were purchased from General Bio (Anhui) Co. CCLP-1 and HuH-28 cells were spread into 6-well plates at 1×10^5 cells/well, and CCLP-1 cells were transfected with miR-ESCO2 and miR-NC, and HuH-28 cells were transfected with sh-ESCO2 and sh-NC according to the Lipofectamine 3000 (Invitrogen) reagent instructions.

Detection of cell proliferation by methylthiazolyldiphenyl-tetrazolium bromide (MTT) assay

CCLP-1 and HuH-28 cells were digested using trypsin, counted and added to 96-well plates (1×10^4/mL) and incubated in the incubator until the cells were adherent to the wall. After 0, 12, 24, 49, and 72 h, respectively, 20 µL of 0.5% MTT (Solarbio, M1020) reagent was added and incubated for 4 h in the incubator. Dimethyl sulfoxide 150 µL was added to fully dissolve, and the absorbance value of each well was measured after 10 min, and the result was taken as the average of each compound well.

Cell clonogenic assay

Digest CCLP-1 and HuH-28 cells with trypsin and count them. Add the cell suspension at 500 cells per well to a 6-well plate. Place the 6-well plate in the incubator for continued culture for 1–2 weeks. When the formed colonies meet experimental criteria, remove the 6-well plate. Wash three times with phosphate-buffered saline (PBS), then add pre-chilled methanol solution to each well and incubate at room temperature for 20 minutes. Discard the supernatant. After washing with PBS, add 1% crystal violet solution to each well and stain at room temperature for 15 minutes. Recover the stained solution. Rinse the 6-well plate slowly under running water. Allow to air dry, then photograph, count, and perform statistical analysis.

Transwell assay for detecting cell invasion

Dilute Matrigel (Corning, 354234, New York, USA) with DMEM medium at a 1:8 ratio and coat the upper chamber surface of the Transwell chamber (Corning, 3422). Incubate at 37 ℃ for 30 minutes. Add 750 µL DMEM medium containing 20% fetal bovine serum to the lower chamber of the Transwell, and add 200 µL cell suspension at a density of 1×10^5 cells/mL to the upper chamber. Incubate in a cell culture incubator for 48 hours, then fix with methanol, stain with 0.3% crystal violet for 15 minutes, and wash three times with phosphate-buffered saline. Wipe off cells from the upper surface of the chamber using a cotton swab. Observe under a microscope at 200× magnification. Randomly select three fields of view, count the cells, and calculate the average value.

Detection of apoptosis by annexin V-PI assay

CCLP-1 and HuH-28 cells were placed in 6-well plates at a cell density of 1×10^6/mL, and after overnight incubation in an incubator, the cells were trypsin-digested and washed with phosphate buffer. Add binding buffer, ice bath, take 5 µL of Annexin V-FITC and 10 µL of propidium iodide (PI) (FineTest, K019) in cell suspension, mix well and then stain for 10 min at 4 ℃ away from light. 490 µL of binding buffer was added, and the cells were left to stand for 1 h away from light, and apoptosis was detected using a flow analyzer (UN, COPAS Infinity).

Mouse model construction and processing

Forty-four BALB/c female mice (6 weeks old) (700000004) were purchased from Wuhan Luobin Life Sciences Technology Co., Ltd. (Animal sex had no effect on the results of this study). CCLP-1 and HuH-28 cell suspensions in good condition were counted and their cell number was adjusted to 1×10^7 cells/mL. Nude mice were randomly divided into miR-ESCO2 (CCLP-1), miR-NC (CCLP-1), sh-ESCO2 (HuH-28), and sh-NC (HuH-28) groups (all n=11), and 200 µL of cell suspensions were withdrawn and slowly injected subcutaneously into the same locations of the four groups of nude mice. Subsequently, the tumors were weighed at 5-day intervals, and the volume of the tumors was measured and calculated periodically. Animal experiment researchers were trained in the theory of animal care or handling and observed the health and behavioral status of the mice on a daily basis and changed the water and bedding every 3 days. After 30 days of observation, no mice died in each group, but significant differential changes in tumor volume were observed in each group. Subsequently, mice (5 mice in each group) were executed by cervical dislocation to minimize pain and discomfort, and the executed mice were dissected to measure tumor volume and weight. In order to further observe the effect of *ESCO2*

overexpression on the survival of mice, the survival of the remaining 6 mice in each group was continued with an observation endpoint of 48 days, after which all mice were executed by cervical dislocation and survival statistics were analyzed. All the experimental procedures were performed under a project license (No. 2024-JR-026) granted by the Beijing Jinglai Huake Biotechnology Co., Ltd. Animal Care and Use Committee, in compliance with the Care and Use of Laboratory Animals for the care and use of animals.

Real-time quantitative polymerase chain reaction (RT-qPCR)

The logarithmic growth phase cells/tissues were digested with TrizoL (Absin, abs9331, Shanghai, China) to extract RNA, and after detecting the concentration and purity of the sample RNA, the reverse transcription reaction of cDNA was carried out by the reverse transcription kit (Yeasen, 11121ES60, Shanghai, China). The qPCR reaction was then performed according to the real-time fluorescence quantitative PCR kit (Yeasen, 13154ES60). A 10 μL reaction system was prepared according to 0.4 μL of each upstream and downstream primer, 10 μL of 2× Master Mix, 0.8 μL of cDNA template, and 8.4 μL of sterilized water. Expression levels were calculated by $2^{-\Delta\Delta Ct}$. The relevant primers were synthesized by Shanghai Biyuntian Biotechnology Co. (Table S2).

Western blot (WB)

Total proteins were extracted from cells/tissues using radioimmunoprecipitation assay buffer lysis buffer (TBD, RIPA20110527, Beijing, China), and protein concentration was determined by bicinchoninic acid (BCA) assay (TIANGEN, PA115-01, Beijing, China). Separation and concentration gels were prepared for electrophoresis using sodium dodecyl sulfate polyacrylamide gel electrophoresis gel kit (Acmec, AP1320, Shanghai, China). Add appropriate amounts of marker and samples, run electrophoresis at 80 V constant voltage for 30 minutes. Transfer the gel to a polyvinylidene fluoride (PVDF) membrane (Elabscience, E-BC-R266, Wuhan, China) at 4 ℃, 300 mA for 90 minutes. Remove the PVDF membrane, briefly rinse with tris-borate-sodium tween-20 (TBST) (NCM Biotech, WB21000, Suzhou, China), then place in blocking solution and gently shake for 1 hour. Incubate PVDF membranes with the following primary antibodies: ESCO2 (Abcam, ab219996, RRID: AB_2924828, 1:500, Cambridge, UK), GAPDH (Abcam, ab59164, RRID: AB_3676490, 1:2,000), and incubated overnight at 4 ℃ on a rocking incubator. Wash three times with TBST on a rocking incubator for 15 min each. Incubate the membrane in secondary antibody dilution buffer (CUSABIO, CSB-PA001501GA01RB, Wuhan, China) at room temperature for 1 h. Wash three times with TBST on a shaking platform for 15 min each. Expose and photograph using enhanced chemiluminescence (Cytiva, RPN2235, Shanghai, China), then analyze the images.

Immunohistochemical staining

Tumor tissue was dehydrated and embedded. After dewaxing and sectioning, antigen retrieval was performed for 15 min, followed by blocking with BCA for 30 min. The primary antibody *ESCO2* was added and incubated overnight at 4 ℃. The secondary antibody (Abcam, ab6721, RRID: AB_955447, 1:1,000) was added and incubated at room temperature for 1 h. Subsequently, add diaminobenzidine and hematoxylin for staining, followed by rinsing with tap water. After dehydration and clearing, mount with neutral resin and examine under a microscope.

Statistical analysis

All microarray data and data variance analyses were analyzed using the package's built-in statistical analyses, and correlation analyses were performed using the Chi-squared test. Statistical analysis was performed using SPSS 22.0 software, and comparisons of groups were analyzed by analysis of variance. *P<0.05, **P<0.01, ***P<0.001 indicate statistically significant differences.

Results

Differential gene analysis and GO functional enrichment and KEGG pathway analysis

After merging and deduplicating the datasets, 15,351 common genes remained. Differential analysis of the dataset by Limma package yielded 1,372 differential genes (available online: https://cdn.amegroups.cn/static/public/tcr-2025-1-2695-1.xlsx). Then using logFC ≥1 & P value <0.05 and logFC ≤−1 & P value <0.05 as the cutoff, a total of 742 up-regulated genes and 630 down-regulated genes were obtained, of which *ESCO2* expression was significantly up-regulated (*Figure 1A* and Figure S1). Finally, the differential genes in the high/low *ESCO2* group were analyzed and 13

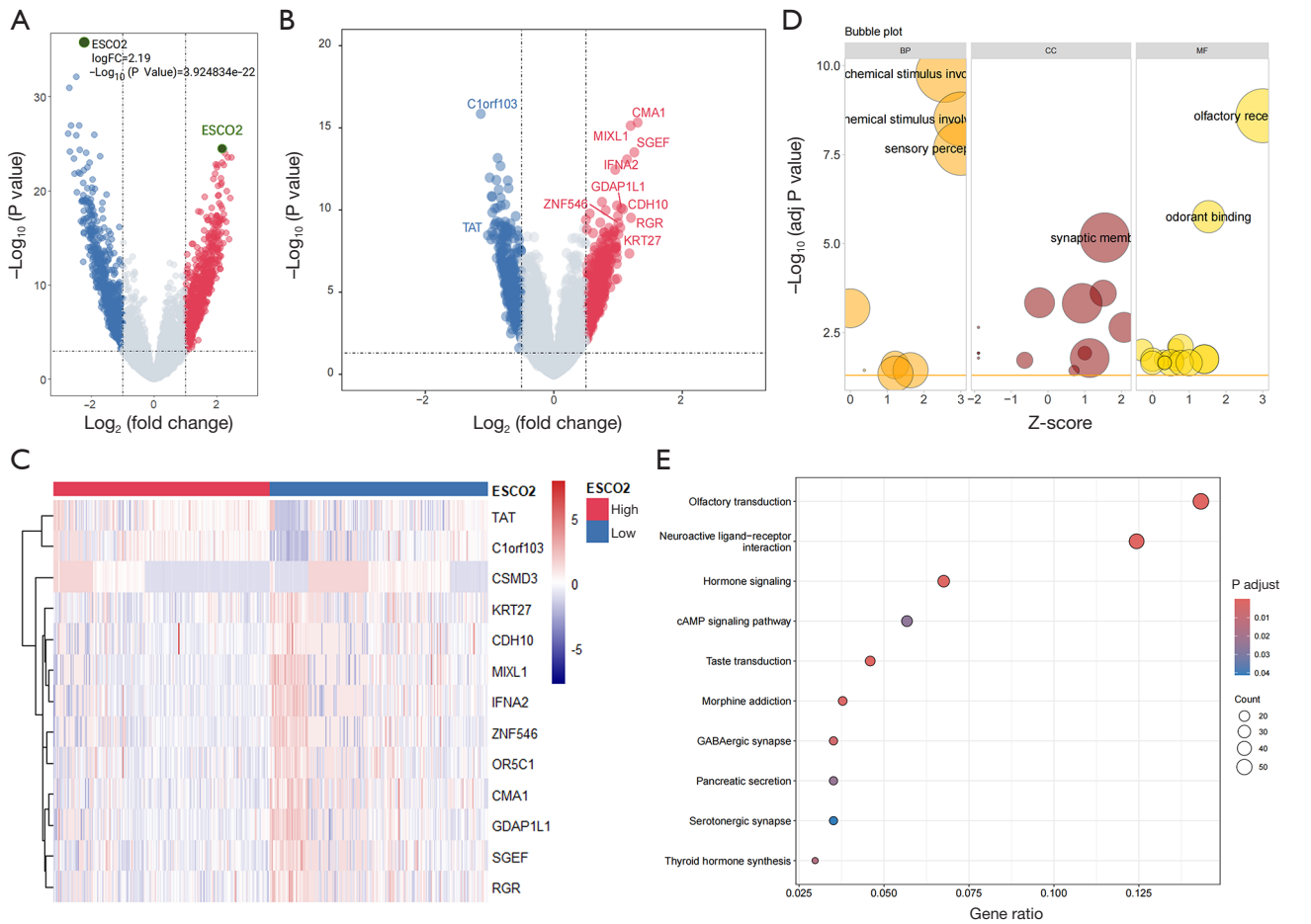

Figure 1 Identification of differentially expressed genes and enrichment analysis plots using GEO data. (A) Volcano plot of differential expression results of CCA tumor samples versus normal samples. Blue indicates "down", gray indicates "stable", and red indicates "up". (B) Volcano plot of differential expression results of high *ESCO2* group versus low *ESCO2* group, grouped according to median *ESCO2* expression value. Blue indicates "down", gray indicates "stable", and red indicates "up". (C) Heatmap of differential expression results between high *ESCO2* group and low *ESCO2* group grouped according to median *ESCO2* expression value. (D) Bubble map of GO enrichment analysis results, each bubble represents a GO term, and different colors represent different GO term types. (E) Bubble map of KEGG enrichment analysis. Among them, the volcano and heat maps label the results with the most significant up- and down-regulation of logFC, with blue color representing low expression and red color representing high expression. BP, biological process; CC, cellular component; CCA, cholangiocarcinoma; *ESCO2*, establishment of sister chromatid cohesion N-acetyltransferase 2; FC, fold change; GEO, Gene Expression Omnibus; GO, Gene Ontology; KEGG, Kyoto Encyclopedia of Genes and Genomes; MF, molecular function; TAT, tyrosine aminotransferase.

differential genes were obtained, including 11 up-regulated genes and 2 down-regulated genes (*Figure 1B,1C*). After obtaining *ESCO2*-related differentially expressed genes, the GO function and KEGG pathway were then enriched and analyzed. The results of GO enrichment analysis are shown in Table S3, and the reticulation (Figure S2A) and bubble plots (*Figure 1D*) suggest that the differentially expressed genes are also involved in the biological processes of detecting chemical stimuli involved in sensory perception, detecting chemical stimuli involved in olfactory perception, and olfactory receptor activity. KEGG pathway results are shown in Table S4, with bubble plots (*Figure 1E*) and circle plots (Figure S2B) suggesting that olfactory conductance, neuroactive ligand-receptor interactions, taste conductance, hormone signaling, morphine addiction, and GABAergic synaptic pathways were significantly enriched.

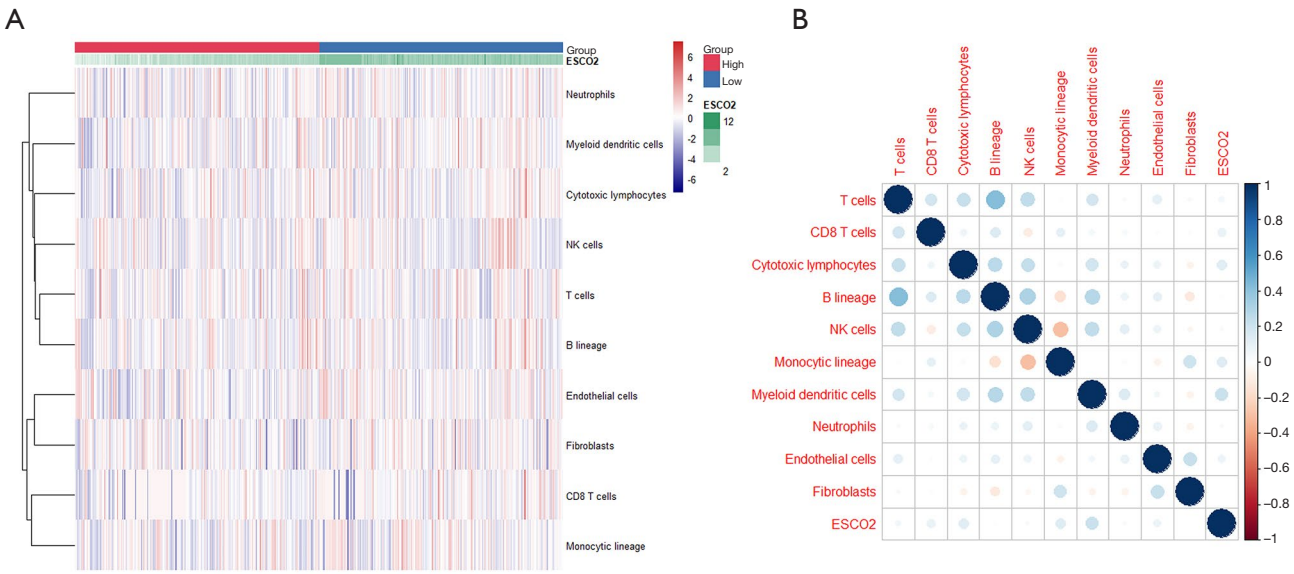

Figure 2 Relationship between *ESCO2* and CCA immune infiltration. (A) Heatmap of the content of 2 stromal cells and 8 immune cells in CCA calculated using MCPcounter. (B) Heatmap of correlation analysis between *ESCO2* and immune infiltrating cells. CCA, cholangiocarcinoma; *ESCO2*, establishment of sister chromatid cohesion N-acetyltransferase 2; NK, natural killer.

Analysis of immune cell infiltration of ESCO2 in CCA patients

The results of the correlation between *ESCO2* and immune cell infiltration revealed that *ESCO2* had the highest correlation with myeloid dendritic cells, monocyte lineage, and cytotoxic lymphocytes (*Figure 2A*,*2B*). The correlation between *ESCO2* and 11 markers in these cells was further explored, and *ESCO2* expression was found to be significantly correlated with the expression of *RASSF4*, *CD1B*, *CD1E*, *CD8A*, *CSF1R*, fibroblast growth factor binding protein 2 (*FGFBP2*), *GNLY*, *KLRC3*, *KLRC4*, *KYNU*, and *PLA2G7* (P<0.05), with significant negative correlation between *CD8A* and *FGFBP2* (Figure S3).

Prognostic value of ESCO2 expression in CCA patients

To evaluate the prognostic value of *ESCO2* in CCA, patients were stratified into high-expression and low-expression groups based on *ESCO2* expression levels. Data from the TCGA were analyzed to assess the correlation between *ESCO2* expression and clinical-pathological parameters. The results showed (Figure S4) that among these factors, age, gender, staging, T-staging, and M-staging were not significantly associated with *ESCO2* expression, and only N-staging had a significant effect on *ESCO2* expression (P<0.05). The prognostic ROC curve for *ESCO2* was then constructed by the Survival ROC package, and *ESCO2* was found to have good predictive accuracy, with the best area under the curve (AUC) value of 0.631 at 5 years (*Figure 3A*). Survival graphs showed a non-significant difference in survival between the two groups (P=0.13, *Figure 3B*). In addition, DFI, DSS, OS, and PFS were lower in patients with high *ESCO2* expression, and DSS, OS, and PFS were significantly correlated with *ESCO2* expression (P<0.05, *Figure 3C-3F*). These results suggest that *ESCO2* may be associated with tumorigenesis and progression.

Results of PPI network visualization of differentially expressed genes

PPI network analysis was performed on *ESCO2*-related differentially expressed genes to explore potential interactions between them. String connectivity graph was drawn and visualized by cytoscape, each node represents a gene, node size and color represent the degree value in the network, degree maps the node color shade, brighter color represents higher degree, then key submodules in the PPI network were extracted and the first 3 key submodules were visualized (Figure S5A-S5D). The main genes found to be more closely associated with the development of *ESCO2* were *IL6*, *FN1*, *GCG*, *H3-4*, *PRKACB*, *PRKACG*, *ADCY5*, *BRCA2*, *CLU*, *SDC1*, and *GNG3* (Figure S5E).

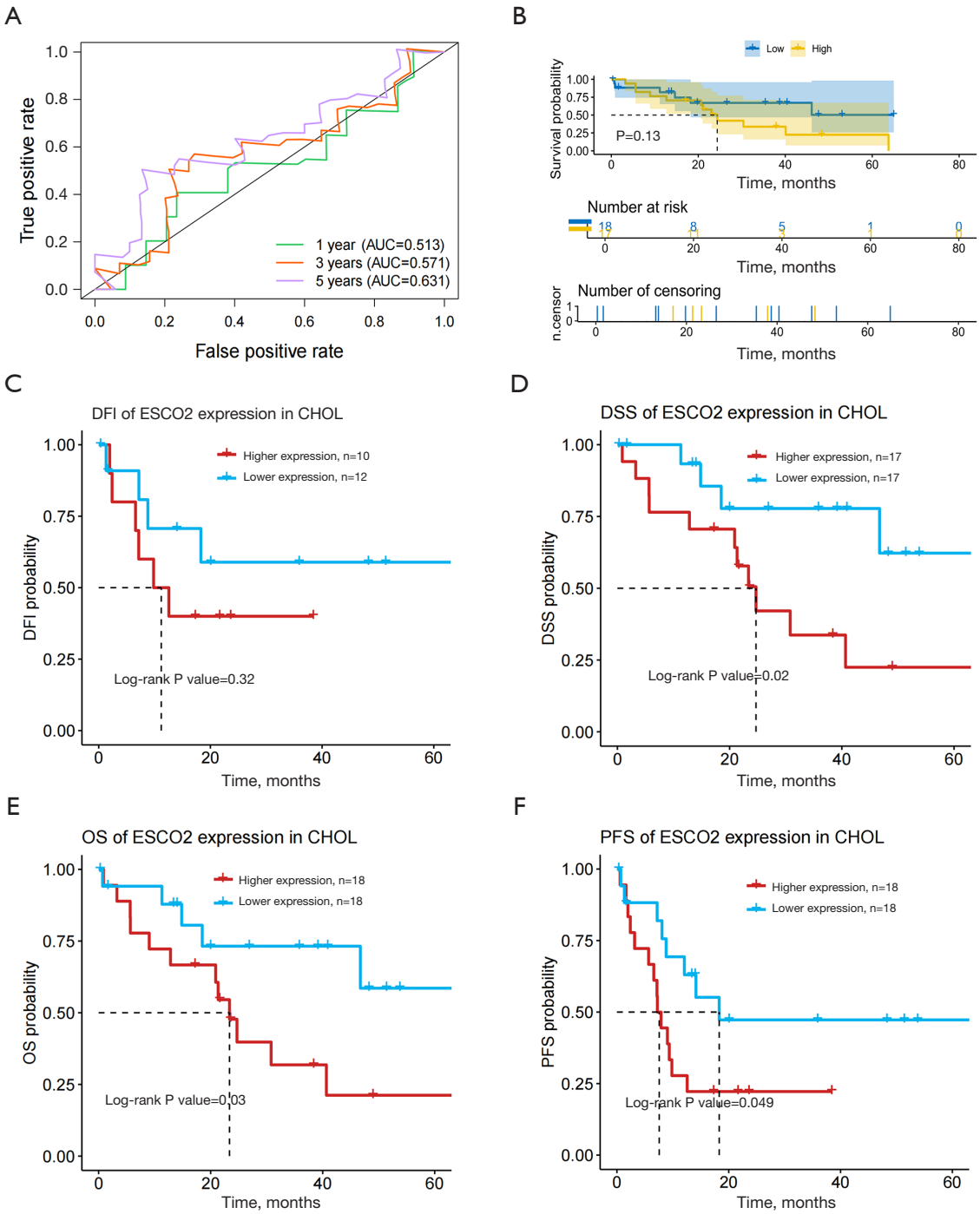

Figure 3 Survival and prognostic analysis of *ESCO2* expression in CCA patients. (A) ROC curve of *ESCO2* identifying CCA prognosis. (B) *ESCO2* survival plot. (C) *ESCO2* survival analysis regarding DFI. (D) *ESCO2* survival analysis regarding DSS. (E) *ESCO2* survival analysis regarding OS. (F) *ESCO2* survival analysis on PFS. AUC, area under the curve; CCA, cholangiocarcinoma; DFI, disease-free interval; DSS, disease-specific survival; *ESCO2*, establishment of sister chromatid cohesion N-acetyltransferase 2; OS, overall survival; PFS, progression-free survival; ROC, receiver operating characteristic.

ESCO2 expression and CNV mutation analysis

The metrics of mutation profiles, mutation counts, genomic alteration scores, and OS were analyzed through the CbioPortal database. The results showed that the *ESCO2* mutation spectrum detected 4% of mutations, mainly missense mutations of unknown significance (Figure S6).

Effect of ESCO2 silencing or overexpression on proliferation, invasion and apoptosis of CCA cells

ESCO2 mRNA expression were analyzed by RT-qPCR in CCA cells, and the results showed that *ESCO2* expression was significantly up-regulated in CCA cells (*Figure 4A*). To investigate the effects of *ESCO2* silencing or overexpression on the biological functions of CCA cells, we first assessed transfection efficiency via WB analysis. Results demonstrated that ESCO2 protein levels were significantly elevated in CCLP-1 cells and significantly reduced in HuH-28 cells (Figure S7). Subsequently, changes in cell viability were first detected by MTT assay. The results showed that the cell proliferation ability of CCLP-1 cells transfected with miR-ESCO2 was significantly increased, and the cell proliferation ability of HuH-28 cells transfected with sh-ESCO2 was significantly inhibited (*Figure 4B*). Clonogenic assays demonstrated that overexpression of *ESCO2* promotes cell growth, while *ESCO2* silencing inhibits cell growth (*Figure 4C,4D*). Transwell assay showed a significant increase in the invasive ability of *ESCO2* overexpressing CCLP-1 cells and a significant decrease in the invasive ability of *ESCO2*-silenced HuH-28 cells (*Figure 4E,4F*). Further staining with Annexin V-PI and analysis by flow cytometry showed that the apoptosis rate of CCLP-1 cells was significantly reduced after *ESCO2* overexpression, while the apoptosis rate of HuH-28 cells was dramatically increased after *ESCO2* silencing (*Figure 4G,4H*). These indicate that *ESCO2* overexpression promotes cell proliferation, migration and inhibits apoptosis.

Effect of ESCO2 silencing or overexpression on tumor growth

Subcutaneous xenografts were established in nude mice to further understand the role of *ESCO2* in CCA growth *in vivo*. The body weight, volume and tumor weight of mice were recorded, and it was found that there was no significant difference in body weight of mice, but the tumor weight and volume of mice in miR-ESCO2 (CCLP-1) group was significantly increased, and the tumor weight and volume of mice in sh-ESCO2 (HuH-28) group was significantly decreased (*Figure 5A-5D*). Survival observations showed eight mice died, all of which died of natural causes. Survival curves showed a significant decrease in the survival rate of mice in the miR-ESCO2 (CCLP-1) group and an increase in the survival rate of mice in the sh-ESCO2 (HuH-28) group (*Figure 5E*). In addition, *ESCO2* overexpression elevated *ESCO2* mRNA levels in tumor tissues, and ESCO2 silencing suppressed *ESCO2* expression (*Figure 5F*). Immunohistochemical analysis revealed that *ESCO2* overexpression increased *ESCO2* expression in tumor tissues, while *ESCO2* silencing reduced *ESCO2* expression in tumor tissues (Figure S8).

Discussion

CCA is a heterogeneous disease with a poor prognosis and an extremely high likelihood of postoperative recurrence and visceral metastasis (28,29). Currently, a variety of targeted drugs and immunotherapeutic drugs are rapidly developing in the clinic, but there are still many challenges in targeted therapy for CCA due to adverse effects, drug resistance, and individual differences (30). Therefore, it is urgent to study the pathogenesis of CCA and related genes. With the development of bioinformatics, by studying the pathogenesis of CCA, new targets can be explored and new treatments can be invented, which will provide significant convenience for patient survival. In this study, a total of 1,372 differentially expressed genes were obtained through screening by utilizing the rich data information of the GEO database, and the up-regulated and down-regulated genes were 742 and 630, respectively. By comparison, it was clear that the gene significantly associated with CCA was *ESCO2*. It was then shown by the TCGA database that the screened gene *ESCO2* was significantly associated with the N-stage of CCA, and the expression of *ESCO2* had a significant effect on the prognostic survival of the patients. Therefore, *ESCO2* can be used as a biomarker for CCA and provide reference value for the diagnosis and prognostic assessment of CCA.

ESCO2 is a pan-cancer biomarker and oncogene that exhibits fairly high levels of expression in 30 tumor tissues, reliably predicts the prognosis of cancer patients, and has also been implicated in cell cycle and proliferation regulation, making it an excellent therapeutic target (31). *ESCO2* has been reported to be overexpressed in breast cancers and has been identified as a prognostic factor in

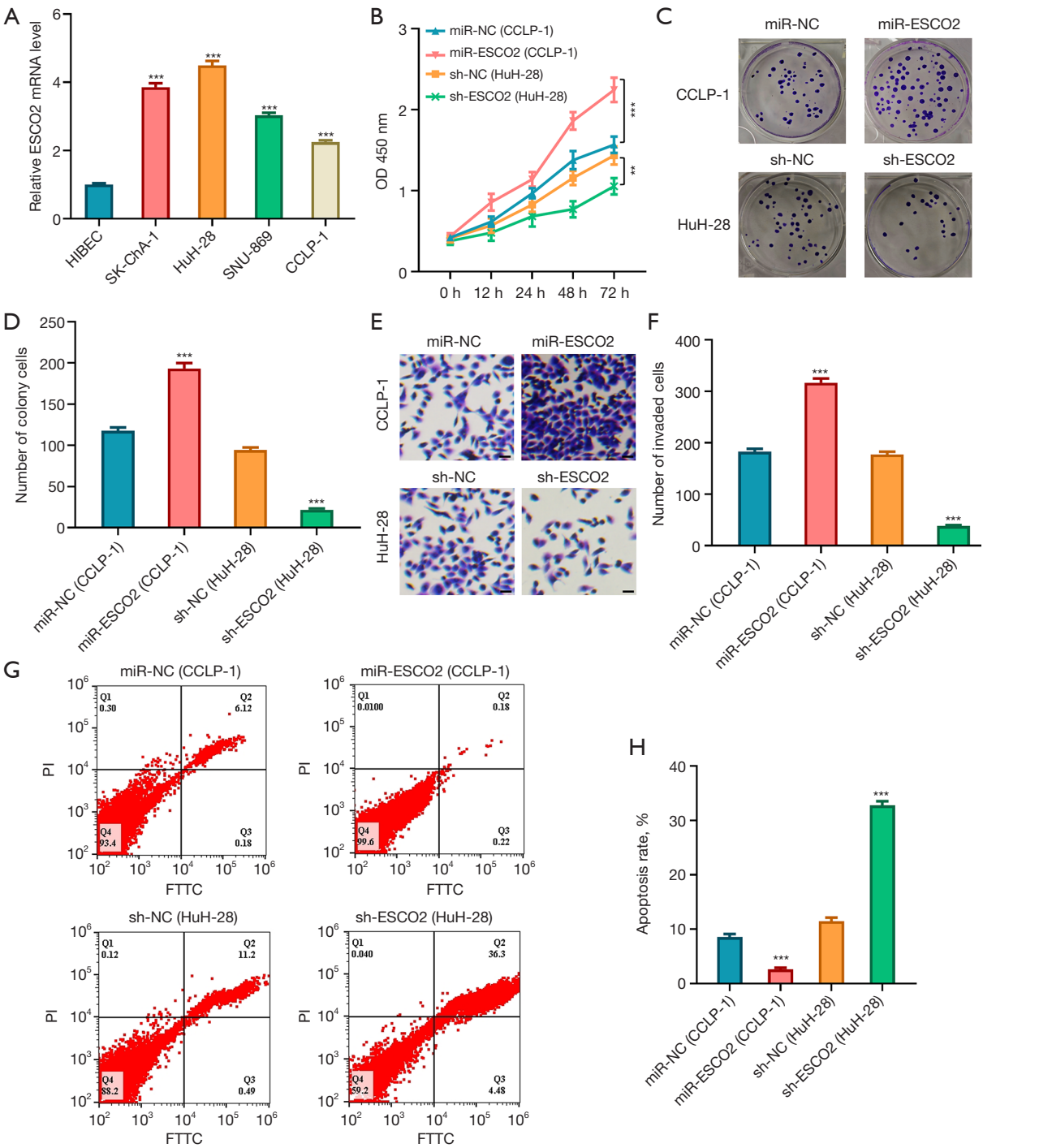

Figure 4 Effects of *ESCO2* silencing or overexpression on CCA cell proliferation, migration and apoptosis. (A) RT-qPCR detection of *ESCO2* mRNA expression level. (B) MTT assay to detect cell proliferation ability. (C,D) Clonogenic assay to assess cell growth. Crystal violet staining. (E,F) Transwell assay to evaluate cell invasion capacity. Crystal violet staining; magnification: 200×. (G,H) Flow assay to detect cell apoptosis rate. **, P<0.01; ***, P<0.001. CCA, cholangiocarcinoma; *ESCO2*, establishment of sister chromatid cohesion N-acetyltransferase 2; FTTC, fluorescein isothiocyanate; MTT, methylthiazolyldiphenyl-tetrazolium bromide; NC, negative control; OD, optical density; PI, propidium iodide; RT-qPCR, real-time quantitative polymerase chain reaction; WB, Western blot.

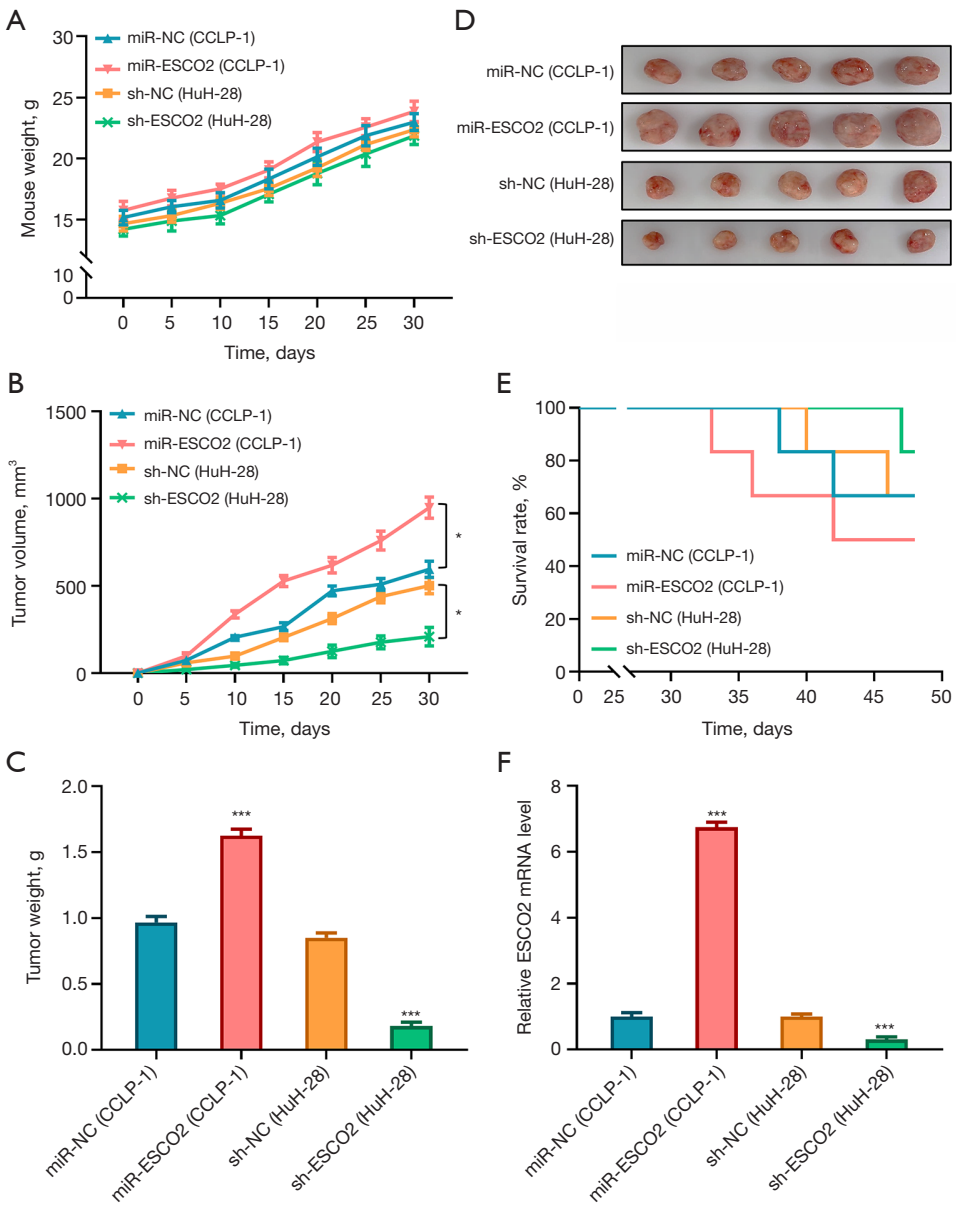

Figure 5 Effects of *ESCO2* silencing or overexpression on tumor growth. (A) Changes in body weight of mice. (B) Mouse tumor volume changes. (C) Mouse tumor weight. (D) Mouse tumor pictures. (E) Mouse survival curves. (F) RT-qPCR detection of *ESCO2* mRNA expression level in tumor tissues. *, P<0.05; ***, P<0.001. *ESCO2*, establishment of sister chromatid cohesion N-acetyltransferase 2; NC, negative control; RT-qPCR, real-time quantitative polymerase chain reaction.

breast cancers (32). Studies have shown that differential expression of *ESCO2* plays different roles in tumors (31). Liu *et al.* (33) showed through database analysis that high *ESCO2* expression is associated with poor prognosis in low-grade gliomas and may play an oncogenic role by affecting cell replication and DNA repair. Zhang *et al.* (34) found that *ESCO2* was overexpressed in renal cell carcinoma and promoted renal cell carcinoma progression by upregulating its expression. However, *ESCO2* expression was down-regulated in esophageal squamous cell carcinoma and correlated with the survival risk of esophageal squamous cell carcinoma, suggesting that *ESCO2* may be a tumor suppressor in esophageal squamous cell carcinoma (35). In addition, studies on

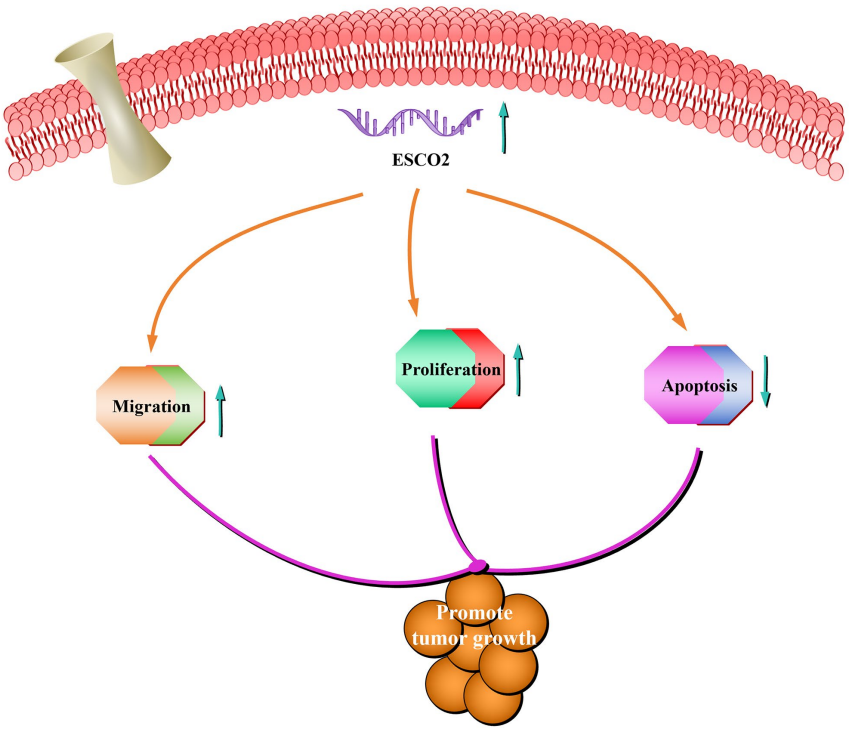

Figure 6 Schematic diagram of *ESCO2* regulation of CCA cell proliferation. CCA, cholangiocarcinoma; *ESCO2*, establishment of sister chromatid cohesion N-acetyltransferase 2.

the regulatory mechanism of *ESCO2* have revealed that *ESCO2* can down-regulate the expression of MIIMP2 by mediating the process of EMT, thereby inhibiting colorectal cancer cell migration and metastasis (36).

The above studies have shown that *ESCO2* expression patterns and regulatory mechanisms in different types of tumors vary greatly. However, its expression and clinical significance in CCA remain unclear. In this study, we found for the first time that *ESCO2* expression was significantly up-regulated in four types of CCA cells. Subsequent up-regulation of *ESCO2* expression in CCLP-1 cells resulted in significantly enhanced proliferation, migration and *in vivo* tumor growth and significantly reduced apoptosis. Silencing *ESCO2* expression in HuH-28 cells showed the opposite effect. The results suggest that *ESCO2* has a significant effect on the malignant biological manifestations of CCA cells and may have potential therapeutic target value.

However, there are some limitations in this study. First, this study lacked the validation of clinical samples, and further clinical samples of CCA patients should be included for validation in the future. Second, the current study is based solely on preliminary investigations using the functional phenotype of *ESCO2*; subsequent research is needed to further elucidate its specific functions and underlying molecular mechanisms. Finally, metastasis experiments *in vivo* after *ESCO2* overexpression/silencing were not performed in this study, and further studies are needed to analyze them in the future to clarify the biological role of *ESCO2* in tumor metastasis *in vivo*. Future studies utilizing clinical cohorts with complete treatment histories are needed to explore the potential of *ESCO2* as a predictive biomarker for treatment response.

Conclusions

In this study, we used bioinformatics combined with gene chip technology to screen and obtain *ESCO2*, a core gene significantly associated with CCA, and *ESCO2* was significantly associated with the prognosis of CCA patients. *ESCO2* has an important biological role in CCA cell proliferation, migration, apoptosis, and tumor growth *in vivo*, and up-regulation of *ESCO2* expression can promote the malignant progression of CCA (*Figure 6*), which provides a new therapeutic target for CCA

treatment.

Acknowledgments

None.

Footnote

Reporting Checklist: The authors have completed the ARRIVE and MADR reporting checklists. Available at https://tcr.amegroups.com/article/view/10.21037/tcr-2025-1-2695/rc

Data Sharing Statement: Available at https://tcr.amegroups.com/article/view/10.21037/tcr-2025-1-2695/dss

Peer Review File: Available at https://tcr.amegroups.com/article/view/10.21037/tcr-2025-1-2695/prf

Funding: None.

Conflicts of Interest: All authors have completed the ICMJE uniform disclosure form (available at https://tcr.amegroups.com/article/view/10.21037/tcr-2025-1-2695/coif). The authors have no conflicts of interests to declare.

Ethical Statement: The authors are accountable for all aspects of the work in ensuring that questions related to the accuracy or integrity of any part of the work are appropriately investigated and resolved. The study was conducted in accordance with the Declaration of Helsinki and its subsequent amendments. All the experimental procedures were performed under a project license (No. 2024-JR-026) granted by the Beijing Jinglai Huake Biotechnology Co., Ltd. Animal Care and Use Committee, in compliance with the Care and Use of Laboratory Animals for the care and use of animals.

References

1. Dixon ME, Williams M, Pappas SG. Cholangiocarcinoma. Cancer Treat Res 2024;192:165-84.
2. Kidanemariam S, Gu J, Yoon JH, et al. Cholangiocarcinoma: Epidemiology and Imaging-Based Review. R I Med J (2013) 2024;107:43-8.
3. Qurashi M, Vithayathil M, Khan SA. Epidemiology of cholangiocarcinoma. Eur J Surg Oncol 2025;51:107064.
4. Ohaegbulam KC, Koethe Y, Fung A, et al. The multidisciplinary management of cholangiocarcinoma. Cancer 2023;129:184-214.
5. Chiablaem K, Jinawath A, Nuanpirom J, et al. Identification of RNF213 as a Potential Suppressor of Local Invasion in Intrahepatic Cholangiocarcinoma. Lab Invest 2024;104:102074.
6. Liu D, Shi Y, Chen H, et al. Molecular profiling reveals potential targets in cholangiocarcinoma. World J Gastroenterol 2023;29:4053-71.
7. Chen Z, Gao J, Li Z, et al. Integrative analysis reveals different feature of intrahepatic cholangiocarcinoma subtypes. Liver Int 2024;44:2477-93.
8. Ma Z, Sun J, Li Z, et al. AMDHD1 acts as a tumor suppressor and contributes to activation of TGF-β signaling pathway in cholangiocarcinoma. Cell Death Differ 2025;32:162-76.
9. Wang Z, Zhang Y, Shen Y, et al. Liquidambaric acid inhibits cholangiocarcinoma progression by disrupting the STAMBPL1/NRF2 positive feedback loop. Phytomedicine 2025;136:156303.
10. Jevitt AM, Rankin BD, Chen J, et al. The cohesin modifier ESCO2 is stable during DNA replication. Chromosome Res 2023;31:6.
11. Sanchez AC, Thren ED, Iovine MK, et al. Esco2 and cohesin regulate CRL4 ubiquitin ligase ddb1 expression and thalidomide teratogenicity. Cell Cycle 2022;21:501-13.
12. Fu J, Zhou S, Xu H, et al. ATM-ESCO2-SMC3 axis promotes 53BP1 recruitment in response to DNA damage and safeguards genome integrity by stabilizing cohesin complex. Nucleic Acids Res 2023;51:7376-91.
13. Guo F, Luo Y, Ye G, et al. Circular RNA METTL15/miR-374a-5p/ESCO2 axis induces colorectal cancer development. Acta Biochim Pol 2023;70:541-9.
14. Chen D, Huang Y, Zhang W, et al. ESCO2 promotes the proliferation of hepatocellular carcinoma through the PI3K/AKT/ mTOR signaling pathway. J Cancer

2025;16:2929-45.
15. Hu J, Yan J, Chen Y, et al. ESCO2 promotes hypopharyngeal carcinoma progression in a STAT1-dependent manner. BMC Cancer 2023;23:1114.
16. Guo W, Zhao S, Yan K, et al. The Potential of ESCO2 as a Prognostic and Immunotherapeutic Marker of Pan-Cancer and Its Role in Anti-PD-1 Treatment of Bladder Cancer. Oncology 2025;103:610-27.
17. Parry WH, Martorano F, Cotton EK. Management of life-threatening asthma with intravenous isoproterenol infusions. Am J Dis Child 1976;130:39-42.
18. Colaprico A, Silva TC, Olsen C, et al. TCGAbiolinks: an R/Bioconductor package for integrative analysis of TCGA data. Nucleic Acids Res 2016;44:e71.
19. Leek JT, Johnson WE, Parker HS, et al. The sva package for removing batch effects and other unwanted variation in high-throughput experiments. Bioinformatics 2012;28:882-3.
20. Law CW, Alhamdoosh M, Su S, et al. RNA-seq analysis is easy as 1-2-3 with limma, Glimma and edgeR. F1000Res 2016;5:ISCB Comm J-1408.
21. Hong W, Yuan H, Gu Y, et al. Immune-related prognosis biomarkers associated with osteosarcoma microenvironment. Cancer Cell Int 2020;20:83.
22. Yu G, Wang LG, Han Y, et al. clusterProfiler: an R package for comparing biological themes among gene clusters. OMICS 2012;16:284-7.
23. Becht E, Giraldo NA, Lacroix L, et al. Estinating the population abundance of tissue-infiltrating immune and stromal celpopulations using gene expression. Genome Biol 2016;17:218.
24. Hong W, Gu Y, Guan R, et al. Pan-cancer analysis of the CASP gene family in relation to survival, tumor-infiltrating immune cells and therapeutic targets. Genomics 2020;112:4304-15.
25. Szklarczyk D, Morris JH, Cook H, et al. The TRlNG database in 2017:quality-controlled protein-protein association networksmade broadly accessible. Nucleic Acids Res 2017;45:D362-D368.
26. Shannon P, Markiel A, Ozier O, et al. Cytoscape: A Software Environment for Integrated Models of Biomolecular Interaction Networks. Genome Res 2003; 13:2498-504.
27. Gao J, Aksoy BA, Dogrusoz U, et al. Integrative analysis of complex cancer genomics and clinical profiles using the cBioPortal. Sci Signal 2013;6:pl1.
28. Hrudka J, Matěj R. Cholangiocarcinoma - Morphology, Immunohistochemistry, and Genetics. Cesk Patol 2025;61:148-58.
29. Izquierdo-Sanchez L, Lamarca A, La Casta A, et al. Cholangiocarcinoma landscape in Europe: Diagnostic, prognostic and therapeutic insights from the ENSCCA Registry. J Hepatol 2022;76:1109-21.
30. Li Y, Yu J, Zhang Y, et al. Advances in targeted therapy of cholangiocarcinoma. Ann Med 2024;56:2310196.
31. Huang Y, Chen D, Bai Y, et al. ESCO2's oncogenic role in human tumors: a pan-cancer analysis and experimental validation. BMC Cancer 2024;24:452.
32. Li P, Wei L, Li M, et al. ESCO2 drives breast cancer proliferation and metastasis through PI3K/AKT/mTOR phosphorylation: A potential therapeutic target. Biochim Biophys Acta Mol Cell Res 2025;1872:120043.
33. Liu Z, Cheng X, Pang B, et al. Effects of ESCO2 or its methylation on the prognosis, clinical characteristics, immune microenvironment, and pathogenesis of low-grade glioma. Int Immunopharmacol 2022;104:108399.
34. Zhang G, Liu SL, Yi WT, et al. Long noncoding RNA ZFPM2-AS1 regulates renal cell carcinoma progression via miR-130a-3p/ESCO2. Kaohsiung J Med Sci 2022;38:530-41.
35. Li G, Lam CY, Chen R, et al. Discovery and validation of proliferative exhausted T cells as a favorable prognostic biomarker in esophageal squamous cell carcinoma. Sci Rep 2025;15:41619.
36. Guo XB, Huang B, Pan YH, et al. ESCO2 inhibits tumor metastasis via transcriptionally repressing MMP2 in colorectal cancer. Cancer Manag Res 2018;10:6157-66.

Cite this article as: Fan L, Jiang Y, Hu J, Xiao F, Chai Y, Yi B, Qiu Y. Carcinogenic role of ESCO2 in cholangiocarcinoma: integration of bioinformatics analysis and experimental validation. Transl Cancer Res 2026;15(5):418. doi: 10.21037/tcr-2025-1-2695